An Experimental Study Followed by a Development and a Comparison of Regression Models for Predicting TJ Electric Discharge in Insulators

Nabila Saim[1*], Ferroudja Bitam-Megherbi[2]
1, 2- Laboratory of Electrical Engineering Advanced Technologies (LATAGE), Faculty of Electrical Engineering and Computer Science, Department of Electrical Engineering, Mouloud Mammeri University, BP 17 RP, Tizi Ouzou, Algeria.
Email: nabila_saim@yahoo.fr (Corresponding author)
Email: ferroudja_megherbi@yahoo.fr

Received: November 2020 Revised: February 2021 Accepted: April 2021

ABSTRACT:
Analyzes of electric discharge are sometimes tedious and relatively expensive. To overcome this problem, some scientists are working on variance analysis projects. The article presents the results of an electric discharge experiment performed on silicone, porcelain and heat tempered glass insulators at Triple Junction (TJ). The objective of this study is to develop a polynomial and Gaussian simple regression model (Polynomial Simple Linear Regression (SLR) model and Gaussian simple nonlinear regression model) considering different parameters by analyzing the observed quantitative data. The dependent variable or variable to be explained (discharge current) is a function of four independent variables (explanatory variables): voltage application time (*t*), solid insulator surface condition: net surface (*t'*), worn rubbed surface with sandpaper (*t''*) and active electrode diameter (*diam*). Indeed, this study sets up precise prediction models generating good estimates of the studied variables values. A polynomial SLR model is proposed capable of predicting electric discharge with an adjusted coefficient of determination (R^2 *adj*) of 0.9774 for *t* and *t'*, 0.9773 for *t''* and 0.9945 for *diam*. While (R^2 *adj*) for the Gaussian model reaches 0.9989 for *t* and *t'*, 0.9998 for *t''*. By considering this, these models are strongly recommended to better understand and characterize the discharge and contribute to the improvement of the insulation and its design for better optimization and high performance.

KEYWORDS: Linear Regression, Maximum Discharge Current, Triple Junction, Electrical Aging, Insulating Surface, Modeling.

1. INTRODUCTION

In armored equipment, Gas Insulated Switchgears (GIS), used in transmission and distribution networks, the reduction of the material size which constitutes it, is a constant demand for production cost issues and better dielectric performance [1]. In these and other conditions, the dielectric performance of The Triple Junction (TJ) depends on several factors: the geometry, the High Voltage (HV) electrodes nature, the insulator surface condition, the voltage application time (*t*) as well as the used insulators dielectric properties [2-3].

TJ is the junction point between an insulator, metal and gas. A strengthening of the field appears, this region is likely to cause the appearance of Partial Discharges (PDs) and attract metal particles [4]. The problems of charge accumulation on the insulation surface can reduce its dielectric strength when applying a specific overvoltage (temporary overvoltage, maneuver shock, lightning shock) [5].

The analysis and understanding of the multitude of complex phenomena that can appear under the presence of HV at TJ becomes necessary for the insulation optimization for better performance [6]. The initiation of discharges from a triple point (insulator, metal, gas) leads to a lowering of the ignition voltage [7]. These produced discharges locally charge the insulation surface, which causes a change in the field distribution in the discharge area and therefore a modification in their regime. The breakdown process is the electric avalanche sequence developing and progressing from the anode to the cathode. In fact, the propagation of the discharges from TJ on the insulation surface follows in a first approximation of the laws of Toepler [8] (relating the propagation distance to the voltage for the two polarities with a different director coefficient). These surface discharges lead to a flashover risk and

Paper type: Research paper
DOI: https://doi.org/10.52547/mjee.15.3.45
How to cite this paper: N. Saim, F. Bitam-Megherbi, **"An Experimental Study Followed by a Development and a Comparison of Regression Models for Predicting TJ Electric Discharge in Insulators"**, *Majlesi Journal of Electrical Engineering*, Vol. 15, No. 3, pp. 45-55, 2021.

therefore to the establishment of a surface arc. This mechanism does not require dielectric breakdown of a solid insulator, but corresponds to the development of a discharge on the creepage line at the insulator surface [9]. It should also be noted that these surface discharges have specific physical properties leading to a fast propagation speed (of the order of 100 km / s - streamers magnitude order) [10]. The development of the avalanche is numerically modeled [11]. Experimental tests of the research predictions are not given here. It is proven both theoretically and experimentally that use of the metal shielding ring can effectively eliminate the flashover problem on the insulating surface from the TJ based on the Secondary Electron Emission Avalanche theory (SEEA). This requires further investigation and research to ensure that the study achieves its objectives in particular on four main axes: quality, time, cost and customer's satisfaction [12]. In addition, L. Zeghichi and al. compared experimental and modeling results based on the Monte Carlo's method in order to simulate the basic phenomena in an electric discharge and the determination of the ambient electric field. This study results can only be used in the oxygen case in a plane-plane electrode system [13]. Otherwise, Junhao Li et al. studied the influence of oil aging and pressed cardboard on the PD characteristics at TJ. The charge, the frequency and the maximum discharge current (I_{max}) were measured during the flashover [14]. The influence of the insulation surface condition and the TJ geometry on the flashover characteristics is discussed. Interactions between the spacer and the discharge development processes in the surrounding gas have not been taken into account [15]. Regression models have been developed and validated for a PD response multivariate system, i.e. average charge, number of discharge pulses, average charge current and the greatest repetitive discharge amplitude over the data acquisition period. However, it remains to validate these models on different equipment installed in a large zone and in the long term [16].

In this work, we will first discuss the experimental study of the electric discharges occurring in the TJ region for a solid insulator surface with or without defects under alternating applied voltage (V). On the other hand, we analyze the effects of the active electrode geometry and the voltage application time (t) on I_{max}. Subsequently, these currents will be modeled by a polynomial and Gaussian simple regression model (Polynomial Simple Linear Regression (SLR) model and Gaussian simple nonlinear regression model). The latter results are from an optimization problem that is easy to solve. The model thus will allow us to organize at best our experimental tests and to expose the parameters that influence the electric discharge. This study should allow us to better understand the complex problems appearing in TJ with a view for optimizing under real conditions for better performance of insulators in industry over both the short and long term.

2. THE CASE STUDY

The tests are carried out in a Faraday cage. The test cell is powered with alternating voltage from a single phase transformer of 100 kV, 50 Hz and 10 kVA. The voltage is variable thanks to a voltage variator that can be seen on the control desk (see Fig. 3).

The HV electrode is a cylindrical stem in Z200 hard steel of 0.6 cm in diameter (*diam*) ending by a cone whose tip has a radius (r) of 0.15 mm and a solid angle of 21.4 °. This electrode has a total length of 19 cm with a straight part of 12 cm and another inclined part of 7 cm with an inclination angle of 135 °. While the plane electrode is a rectangular plate also in Z200 hard steel of 10.4 cm long, 0.7 cm wide, 0.16 cm high whose terminals are rounded to eliminate side effects. The HV electrode is placed on the solid insulator and in parallel with it; the plane electrode is also placed on the solid insulator thus allowing to have only surface discharges oriented in one direction. The samples used are derived from HV insulators in silicone, porcelain and heat tempered glass. The cutting method of these samples and their dimensions are shown in Fig. 1. Before each test, the sample is thoroughly cleaned with alcohol and then dried. The distance between the electrodes (d) and the position of the sample are adjusted by a mechanical system made of polymethyl methacrylate and bakelite (Fig. 2). The current pulses are visualized using a 20 MHz bandwidth memory oscilloscope that we have connected to a plotter. The oscilloscope measures the voltage drop across a 48.6 kW resistor across which the flat electrode is grounded.

The atmospheric conditions in the Faraday cage are maintained practically constant during the tests: the atmospheric pressure is 1010 hPa, the relative humidity is 63.4% and the temperature is 15 ° C. Their measurements are made by a thermohygrometer and a barometer.

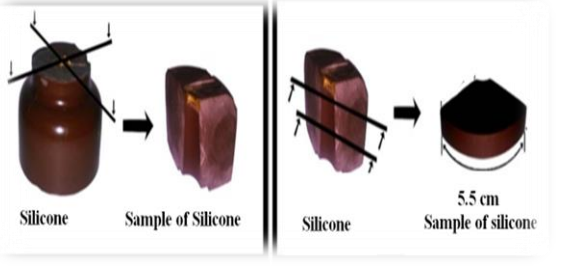

Fig. 1. Dimensions of the samples and their cutting method.

Fig. 2. Tested electrode system.

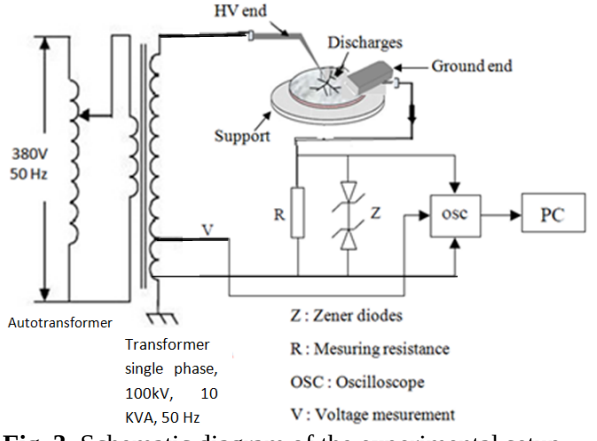

Fig. 3. Schematic diagram of the experimental setup.

3. METHODOLOGY

In this part, a simple regression analysis was performed to predict the effect of *t*, *t'*, *t''* and *diam* on the electric discharge. It is therefore a mathematical modeling of the phenomena studied experimentally.
We give the details of the derivation of our two proposed models. First, the polynomial model, and then the Gaussian.

Let *y* denotes the observed (dependent) variable or variable to be explained. Note that we have n observations which we denote $y_i, \forall\, i = 1, \dots, n$, we assume that each y_i is corrupted by a normal random noise (Gaussian) ε_i of mean and variance equal to 0 and σ^2, respectively. Our main goal is to find a function $f(x)$, where x is the independent variable (explanatory variable), such that $y \cong f(x)$. That is to say, we seek f that minimizes the error between the observations and the proposed model. The choice of f is made based on several criteria. In particular, it is based on the type of the relationship between the depended and the independent variable (linear/nonlinear), and/or the type of the associated optimization problem.

3.1. Polynomial Model

Our first choice for *f* is to be a polynomial function. These models are widely used for the following reasons [17-18-19]:
- The simplicity of the polynomial models form;
- Reasonable flexibility of the polynomial models forms;
- Ease of use of polynomial models computationally;
-The independence of underlying metric of the polynomial models which makes these models a closed family.

Our polynomial is of degree *D*, where $D \geq 2$ is an integer. In this case, the variables to be explained can be written as:

$$y_i = \sum_{j=0}^{D} \beta_i x_i^j + \varepsilon_i, \forall\, i = 1, \dots, n \quad (1)$$

Where, β_i are the coefficients of the polynomial to be determined.
We can further put equation (1) into a compact (matrix) form as follows:

$$y = X\beta + \varepsilon \quad (2)$$

With,

$$y = [y_1 \quad \dots \quad y_n]^T,\ \varepsilon = [\varepsilon_1 \quad \dots \quad \varepsilon_n]^T \ and$$

$$X = \begin{bmatrix} 1 & x_1 & x_1^2 & \dots & x_1^D \\ 1 & x_2 & x_2^2 & \dots & x_2^D \\ \vdots & \vdots & \vdots & \ddots & \vdots \\ 1 & x_n & x_n^2 & \dots & x_n^D \end{bmatrix} \quad (3)$$

Where, $(.)^T$ is the transpose of a vector/matrix. The matrix X of size $(n \times D + 1)$ is assumed to be full-column rank with $n \geq D + 1$.
According to the equation (2) and the above assumptions on ε and X, minimizing the error between y and $X\beta$ is equivalent to solve the following well-known least square problem:

$$argmin_\beta \|y - X\beta\|_2^2 \quad (4)$$

The solution of the optimization problem in equation (4) is the pseudo-inverse given by:

$$\beta^* = \mathrm{X^T(X^TX)^{-1}} \quad (5)$$

By applying the general equation (1) to our case study, we obtain the polynomial models of degree *D* = 7 for *x* = *t*, *x* = *t'* and *x* = *t''* and *D* = 2 for *x* = *diam* corresponding to the dependent variable *y* = I_{max} and this for the three selected materials silicone, porcelain and heat tempered glass. The coefficients of the same model are different and they are different from one independent variable to another and from one material to another.

Besides, for *x* = *t*, *x* = *t'* and *x* = *t''*, the degree of the polynomial models is high (7) and the associated number of estimated terms is also high (8). These

polynomials have oscillations between perfectly associated dimension values. Their interpolating property is bad; moreover these functions are not localized (global non-localized function). Therefore, the polynomial model may lack precision when the function to be modeled presents some severe nonlinearities. Therefore, the use of rational functions such as the Gaussian for modeling can give a good adjustment.

3.2. Gaussian model

There are many physical phenomena that follow a Gaussian distribution, which is why these functions are widely used. In addition, these functions have major advantages such as their central limit theorem as well as the Gaussian function which is the Fourier transform of a Gaussian function [20-21].

We propose the Gaussian function f given by equation (6):

$$f(x;\ \alpha) = \alpha_0 + \ exp\left(\frac{-(x-\alpha_1)^2}{{\alpha_2}^2}\right) + \ exp\left(\frac{-(x-\alpha_3)^2}{{\alpha_4}^2}\right) \quad (6)$$

Where,

$$\alpha = \ [\alpha_0 \quad \dots \quad \alpha_4]^T \quad (7)$$

As in the polynomial case, our variables to be explained can be written in a matrix form as follows:

$$y \ = \ F(x;\ \alpha) + \ \varepsilon \quad (8)$$

With,

$$F(x,\alpha) = \begin{bmatrix} f(x_1;\alpha) \\ \vdots \\ f(x_n;\alpha) \end{bmatrix} \quad (9)$$

It remains now to determine the coefficients vector α. we can do it by solving the following optimization problem:

$$argmin_\alpha \|y - F(x;\alpha)\|_2^2 \quad (10)$$

Compared to equation (4), the optimization problem in equation (10) is more difficult. It has no analytic solution. Furthermore, it is not convex. Thus, we try to solve it approximately using some known algorithms such as Levenberg-Marquardt algorithm [22], which we use in this paper. We should mention, however, that this algorithm (like other ones) is not guaranteed to find the exact optimal solution of equation (10). Nevertheless, it turns out that it works well in practice and it usually successes to find a good approximate solution.

By adapting the Gaussian function developed above (Equation (6)) to our work, we obtain the Gaussian models for $y = I_{max}$ corresponding to $x = t$, $x = t'$ and $x = t''$ for the three materials studied (silicone, porcelain and heat-tempered glass).

The coefficients of these models are not equal in the same model and they differ from one variable x to another and from one material to another.

4. RESULTS AND DISCUSSION

4.1. Experimental Results Analysis

Fig. 4 represents the variation of I_{max} as a function of t for the three selected materials. V = 12 kV was applied to the solid insulation for d = 2.9 cm during 4 hours without interruption and the I_{max} measurement is carried out every Δt = 30 min.

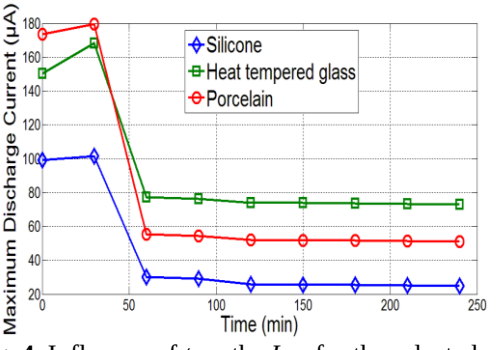

Fig. 4. Influence of t on the I_{max} for the selected materials. Active electrode without defect r = 0.15 mm and *diam* = 6 mm, net insulating surface, V = 12 kV, d = 2.9 cm. ($x = t$).

We observe in Fig. 4 that the I_{max} increases for the first period of electrical aging. From this period on, the discharge current decreases, but the rate of decrease is greater for silicone than for heat tempered glass and porcelain.

During the first period of electrical aging, the three materials were subjected to an electric discharge undergo degradation which results in the breaking of some chemical bonds, the formation of the OH carboxylic group and a significant development of the trees on the surface (the trees length grows with t) which could favor superficial electrical conduction and consequently the increase of I_{max} [23].

On the other hand, this degradation of the three materials is observed visually and consists in the appearance of a moisture layer and a whitish crown. The intensity and thickness of the whitish crown and the humidity quantity observed on the surface are all the more important as t is high.

Moreover, on the second part of electrical aging, the reduction in I_{max} after more than 30 minutes of electrical aging for the three materials, is due to a deposit of humidity, itself consecutive to a degradation

of the electrical surface. This degradation facilitates the electronic bond and the predominance on ionic activity. This electronic link in turn slows down the discharge regime, hence the extinction of this discharge [24].

On the other hand, it was clearly observed that the I_{max} of porcelain is higher than that of heat tempered glass and silicone. This means that the electric aging time has a greater influence on porcelain than on heat tempered glass and silicone, which can be explained by the fact that porcelain is more permeable to the propagation phenomena of electric discharges which can be related to the chemical structure. In other words, porcelain has a weak bonding force between its molecules, unlike heat tempered glass and silicone (silicone has a strong bonding force between its molecules made from oxygen and silicon). Thus, this chemical structure plays a main role in the electrical and dielectric properties of these materials [25].

Fig. 5 shows the variation of I_{max} measured every Δt = 30 min during four hours of t continuously on the solid insulation (three materials: silicone, porcelain and heat tempered glass) for $x = t'$ and $x = t''$. The experiments take place under V = 12 kV and d = 2.9 cm.

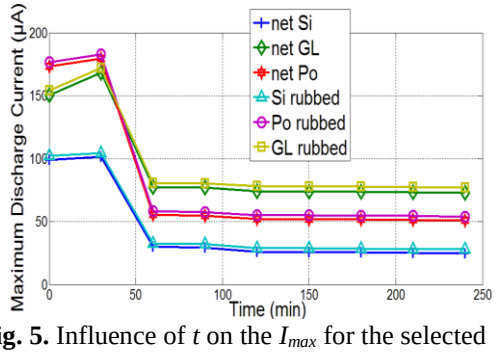

Fig. 5. Influence of t on the I_{max} for the selected materials for a solid insulator with net surface, then with a rubbed surface. Active electrode without defect. r = 0.15 mm and *diam* = 6 mm, V = 12 kV, d = 2.9 cm. ($x = t'$ and $x = t''$).

For the three materials studied (Fig. 5), we notice that increasing t up to 30 minutes leads to an increase in I_{max}. Beyond 30 min, a decrease in I_{max} is observed by increasing t. This is more important for silicone than heat tempered glass and than porcelain; this is valid regardless of the solid insulation surface condition ($x = t'$ and $x = t''$). The same phenomena have been observed and explained for Fig. 4.

In addition, we observe that the currents values of I_{max} of the three samples are larger for $x = t''$ compared to $x = t'$. This is explained by the following phenomenon: the surface worn and rubbed with sandpaper has homogeneity defects, cavities, inclusions of foreign particles, etc. As a result, electric discharges arise in the vicinity of these defects. As soon as the electric field becomes great enough, these discharges can create by erosion, localized fusion, induced chemical transformations or other processes in the insulation, networks of channels more or less conductive called "trees". The trees evolve along with time, thus increasing the electric discharge and consequently the I_{max}. As soon as the size of these trees becomes sufficient, they cause an electrical breakdown [26-27]. Furthermore, the experimental results obtained by J. Lewis [28] show that polishing the solid insulator surface improves the system dielectric strength. The discharge occurs under the form of a channel polished surfaces and under the diffuse form on rough surfaces.

The variation of I_{max} as a function of different HV electrode *diam* for d = 2.9 cm, V = 12 kV and this for the three samples is shown in Fig. 6.

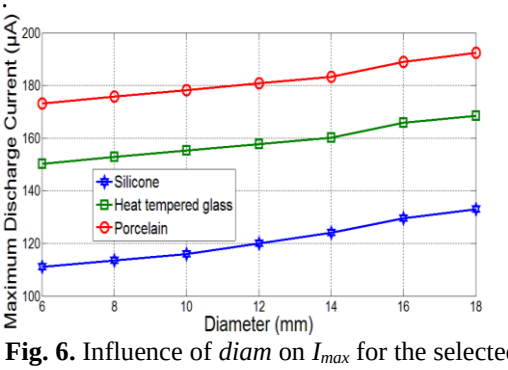

Fig. 6. Influence of *diam* on I_{max} for the selected materials. Active electrode without defect. r = 0.15 mm, net insulating surface, V = 12 kV, d = 2.9 cm. (x = *diam*).

For the three materials studied, Fig. 6 shows that when the *diam* decreases, the I_{max} follows.

When we increase *diam*, therefore HV end surface increase, its resistance (from equation (11)) decreases. As a result, according to Ohm's law (Equation (12)), we observe an increase in the current flowing from this conducting electrode [29-30-31].

$$R = r_0 \, l / S \tag{11}$$

$$I = U/R \tag{12}$$

Where, r_0 is the resistivity (Ω.m), l the length (m) and S is the section (m^2).

4.2. Analysis of the Modeling esults

Figs. 7, 9, 11, 13, 8, 10 and 12 permit to compare the I_{max} obtained from the experiments performed and the polynomial SLR model for $x = t$, $x = t'$, $x = t''$ and x = *diam* as well that of the Gaussian model for $x = t$, $x = t'$ and $x = t''$ in order.

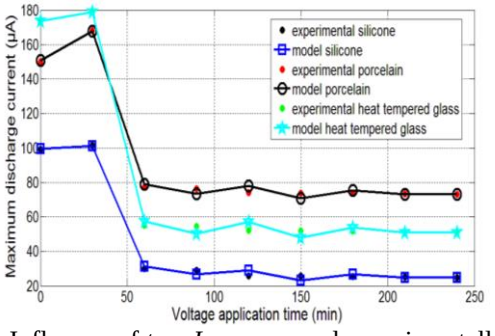

Fig.7. Influence of t on I_{max} measured experimentally and calculated from the polynomial SLR model for the selected materials. Active electrode without defect. r = 0.15 mm and *diam* = 6 mm, net insulating surface, V = 12 kV, d = 2.9 cm. ($x = t$).

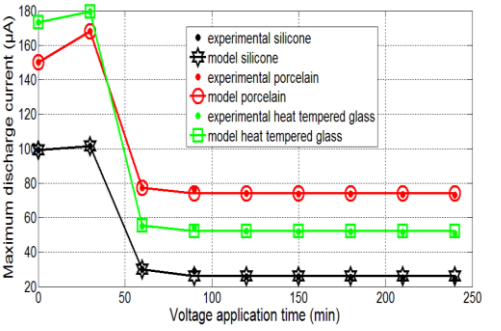

Fig. 10. Influence of t on I_{max} measured experimentally and calculated from the Gaussian model for materials selected for a net surface. Active electrode without defect. r = 0.15 mm and *diam* = 6 mm, V = 12 kV, d 2.9 cm ($x = t'$).

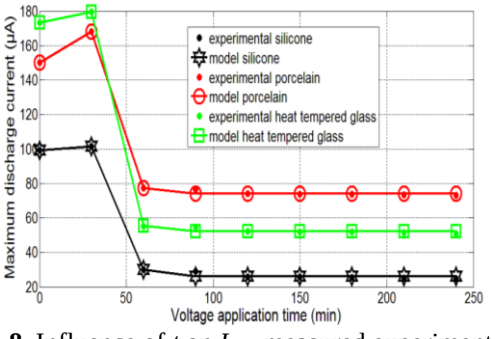

Fig. 8. Influence of t on I_{max} measured experimentally and calculated from the Gaussian model for the selected materials. Active electrode without defect. r = 0.15 mm and *diam* = 6 mm, net insulating surface, V = 12 kV, d = 2.9 cm ($x = t$).

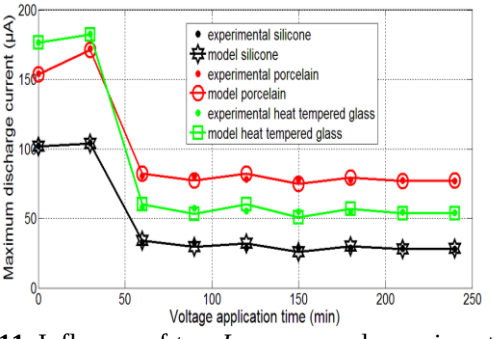

Fig. 11. Influence of t on I_{max} measured experimentally and calculated from the polynomial SLR model for the materials selected for a surface rubbed. Active electrode without defect. r = 0.15 mm and *diam* = 6 mm, V = 12 kV, d = 2.9 cm ($x = t''$).

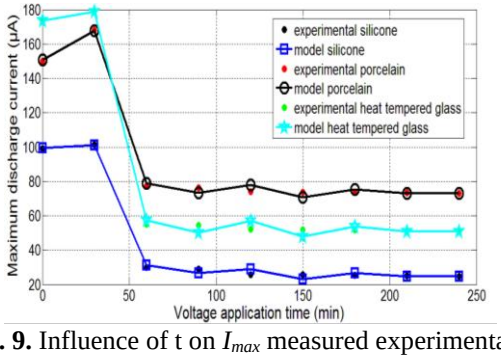

Fig. 9. Influence of t on I_{max} measured experimentally and calculated from the polynomial SLR model for the materials selected for a net surface. Active electrode without defect. r = 0.15 mm and *diam* = 6 mm, V = 12kV, d = 2.9 cm ($x = t'$).

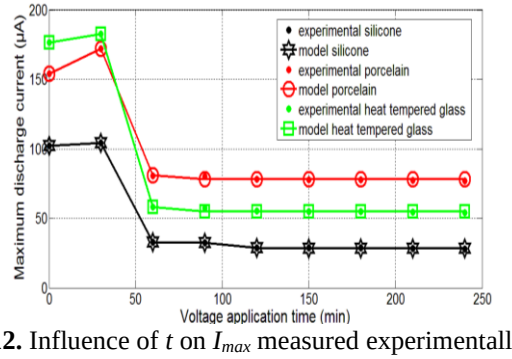

Fig. 12. Influence of t on I_{max} measured experimentally and calculated from the Gaussian model for the materials selected for a surface rubbed. Active electrode without defect. r = 0.15 mm and *diam* = 6 mm, V = 12 kV, d = 2.9 cm ($x = t''$).

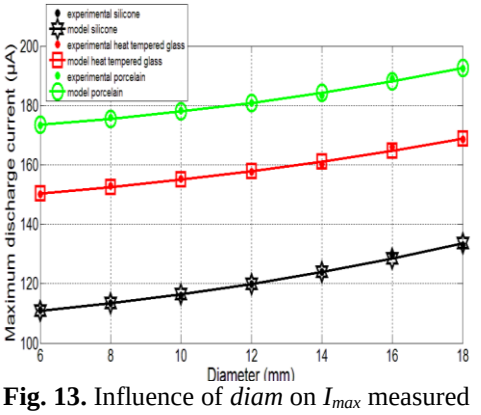

Fig. 13. Influence of *diam* on I_{max} measured experimentally and calculated from the polynomial SLR model for the selected materials. Active electrode without defect. r = 0.15 mm, net insulating surface, V = 12 kV, d = 2.9 cm (x = *diam*).

In addition, the following metrics are calculated and represented in Table 1 for each variable, material and model obtained, for a better understanding and characterization of the prediction model developed [32].

• The coefficient of determination R^2 *adj*

R^2 *adj* is given by the following equation:

$$R^2 = 1 - \frac{\sum_{i=1}^{n}(y_i - \widehat{y_i})^2}{\sum_{i=1}^{n}(y_i - \bar{y})^2} \quad (13)$$

The closer R^2 *adj* is to 1, the better the regression adjustment the data set.

• The mean absolute percentage error *MAPE* (%):

MAPE (%) is given by the following equation.

$$MAPE = \frac{\sum_{i=1}^{n}|\widehat{y_i} - y_i|}{n} \quad (14)$$

MAPE gives better information on the prediction quality. The lower the values are the better is the adjustment.

• The mean square error *RMSE*

RMSE is given by the following equation:

$$RMSE = \sqrt{\frac{\sum_{i=1}^{n}(\widehat{y_i} - y_i)^2}{n}} \quad (15)$$

RMSE tells us about the dispersion or instability of the prediction quality.

Where, n is the number of data, y_i is the value of the i th data, $\bar{y}$ is the data values average and $\widehat{y_i}$ is the value of the i th prediction.

Table 1. Error statistics of Gaussian and polynomial simple regression models obtained in this study.

Parameter	Value														
	Polynomial SLR model									Gaussian model					
	$x = t$ and $x = t'$			$x = t''$			x = *diam*			$x = t$ and $x = t'$			$x = t''$		
	Si	G	Po	Si	G	Po	Si	G	Po	Si	G	Po	Si	G	Po
RMSE (µA)	5.206	6.257	8.22	5.347	6.392	8.248	0.6111	0.8175	0.6677	2.438	1.873	1.837	0.4633	1.771	1.894
MAPE (%)	27.11	39.15	67.56	28.59	40.85	68.02	1.494	2.673	1.783	11.89	7.013	6.746	0.4292	6.272	7.172
R^2 *adj* (-)	0.9744	0.9724	0.9774	0.973	0.971	0.9773	0.9945	0.9852	0.9907	0.9944	0.9975	0.9989	0.9998	0.9978	0.9988

Where: Si, G, Po are respectively silicone, heat tempered glass and porcelain.

According to Table 1, for $x = t$, $x = t'$ and $x = t''$, we see that the Mean Absolute Percentage Error (*MAPE)* (%) is acceptable for both models (polynomial and Gaussian) but even more suitable for Gaussian: A mean absolute percentage error of less than 12% was observed for the latter (see Table 1), furthermore the polynomial model presents outliers (67.56 et 68.02%) which are generally due to measurement errors.

However, for x = *diam*, the mean absolute percentage error is also quite limited 2.673% (see Table 1) and this applies of course to the polynomial SLR model obtained in this study.

Figs. 7 to 13 and Table 1 show that the quality of the results of the prediction models developed (polynomial and Gaussian) is valuable. In other words, the values predicted by the models are fairly close to the true values. Nevertheless, the precision, robustness and the rigor of the Gaussian model (case where $x = t$, $x = t'$ and $x = t''$) are really better. This led us to test and validate the Gaussian model obtained in the study (Gaussian model obtained for $x = t$, $x = t'$ and $x = t''$ from the general equation (6)) for $x = t$, $x = t'$ and $x = t''$ as well as the polynomial SLR model obtained (polynomial model of degree D = 2 obtained for x = *diam* from the general equation (1)) for x = *diam*.

4.3. Models Validation

The metrics mentioned and calculated above, are

unfortunately not sufficient for the prediction precision. The validation of the model to be set up is an essential phase to show that the model is reliable and relevant [33-34]. To do this, the data set was divided into two groups, one for creating the regression model, while the other is used for validating the model by testing it. The values of the input variables used to test and validate the Gaussian model obtained in the study (Gaussian model obtained for $x = t$, $x = t'$ and $x = t''$ from the general equation (6)) for $x = t$, $x = t'$ and $x = t''$ as well as the polynomial SLR model obtained (polynomial model of degree $D = 2$ obtained for $x = diam$ from the general equation (1)) for $x = diam$ are given in Table 2.

Table 2. Input variables for validation of the two Gaussian and polynomial simple regression models.

Model to be validated	Explanatory variable	Range of values
Gaussian	$x = t$ (min)	[270 300 330 360 390 420 450 480 510 540 570 600]
	$x = t'$ (min)	[270 300 330 360 390 420 450 480 510 540 570 600]
	$x = t''$ (min)	[270 300 330 360 390 420 450 480 510 540 570 600]
Polynomial	$x = diam$ (mm)	[20 21 22 23 24 25 26 27 28 29 30 31]

Figs. 14, 15, 16 and 17 compare I_{max} measured experimentally and calculated from the model in order to test and validate the Gaussian model obtained in the study (Gaussian model obtained for $x = t$, $x = t'$ and $x = t''$ from the general equation (6)) for $x = t$, $x = t'$ and $x = t''$ as well as the polynomial SLR model obtained (polynomial model of degree $D = 2$ obtained for $x = diam$ from the general equation (1)) for $x = diam$ respectively.

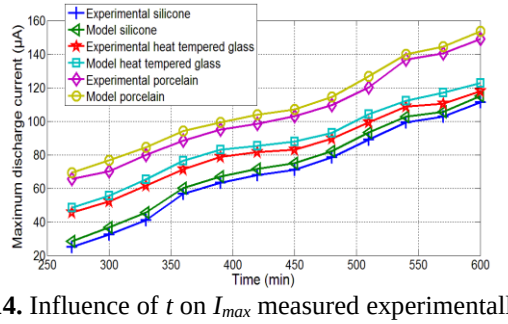

Fig. 14. Influence of t on I_{max} measured experimentally and with a Gaussian model for the selected materials. Active electrode without defect. $r = 0.15$ mm and $diam = 6$ mm, net insulating surface, $V = 12$ kV, $d = 2.9$ cm ($x = t$).

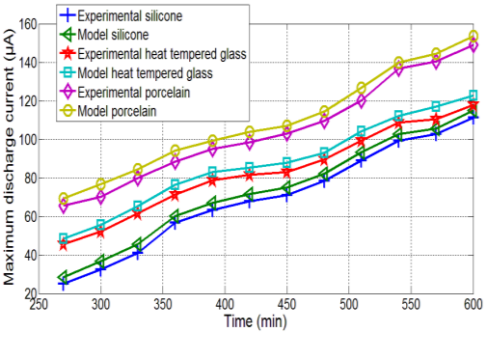

Fig. 15. Influence of t on I_{max} measured experimentally and with a Gaussian model for the materials selected for a solid insulator with net surface. Active electrode without defect. $r = 0.15$ mm and $diam = 6$ mm, $V = 12$ kV, $d = 2.9$ cm ($x = t'$).

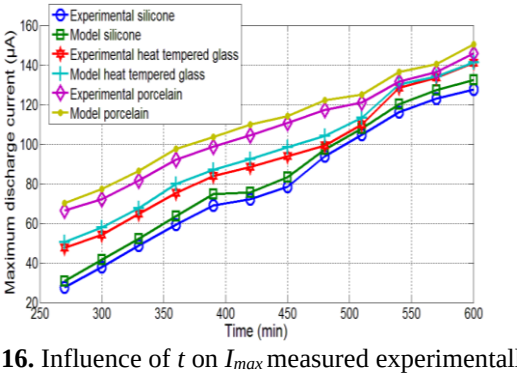

Fig. 16. Influence of t on I_{max} measured experimentally and with a Gaussian model for the materials selected for a solid insulator with a surface rubbed. Active electrode without defect. $r = 0.15$ mm and $diam = 6$ mm, $V = 12$ kV, $d = 2.9$ cm ($x = t''$).

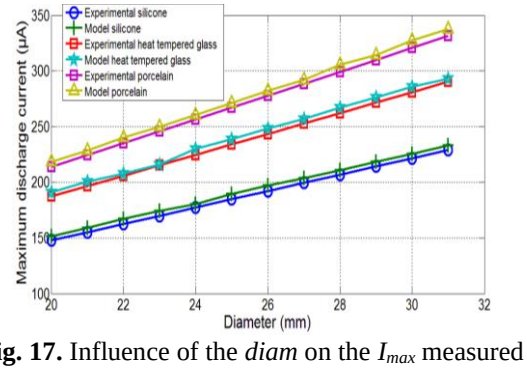

Fig. 17. Influence of the $diam$ on the I_{max} measured experimentally and with a polynomial SLR model for the selected materials. Active electrode without defect. $r = 0.15$ mm, net insulating surface, $V = 12$ kV, $d = 2.9$ cm ($x = diam$).

We can note that the curves of I_{max} (Figs. 14 to 17) according to the simple regression models developed (Gaussian and polynomial) and the experimental tests are very close whatever the explanatory variable, the

model and the material studied.

The results obtained show that the models developed in this study: Gaussians (Gaussian model obtained for $x = t$, $x = t'$ and $x = t''$ from the general equation (6)) and polynomial (polynomial model of degree $D = 2$ obtained for $x = diam$ from the general equation (1)) are validated. Hence, these models are indeed able to predict the values of variable to be explained with precision.

5. CONCLUSION

In this study, we have shown from our experimental results that the mechanism of the surface electric discharge between two electrodes (tip and plane) on insulators samples (silicone, porcelain and heat tempered glass) at the triple junction evaluated by measurements of the maximum current is governed by electrical aging (voltage application time) and solid insulator surface condition as well as the active electrode diameter.

Indeed, electrical aging greatly impacts insulation. This noticeable degradation of the dielectric surface is characterized by an increase in the discharge current for the first period of aging. The space charge accumulated on the dielectric surface is the most suspected factor in this influence. The deposition of substantial moisture layers following intensive aging of the samples appears to be responsible for the decrease in current over the second period. In addition, the discharges level depends on the high voltage electrode diameter; it is larger in the case of a large diameter. In addition, the solid insulation surface condition appears to have a great influence on the pre-breakdown characteristics. The current on polished surfaces is lower than on rough surfaces.

In precision HV, and to predict the values of the variable to be explained (more than often this variable is expensive or time-consuming to acquire), we developed a simple regression model that correctly estimates this variable and describe the discharge phenomena studied experimentally.

Indeed, four explanatory variables (voltage application time, net surface condition, worn surface condition, and diameter) were assimilated as inputs from polynomial and Gaussian simple regression model (Polynomial simple linear regression model and Gaussian simple nonlinear regression model) accurately predicting the electric discharge current. The coefficient of determination R^2 *adj* is limited to 0.9774, 0.9773, and 0.994 for the polynomial model. While that R^2 *adj* limit is 0.9989 and 0.9998 for the Gaussian model which demonstrates that 97.74, 97.73, 99.4, 99.89 and 99.98% of the electric discharge variation is justified by the variation of four explanatory variables for the polynomial model and three explanatory variables for the Gaussian one obtained in this study.

Gaussian models for independent variables: time and clean/worn surface condition as well as the polynomial model for the diameter explanatory variable have better predictions. That is why we put them in place and tested and validated them.

The models proposed are very reliable based on a reduced number of experiments whose main purpose is the electric discharge optimization. These models are a form of energy and finance saving. They provide the industry with information and guidance on making the right choice on insulator technology, while bringing particular attention to its design presenting the best cost /time savings/ expected performance ratio.

The remedies for electric discharge at triple junction on insulating surfaces are the following

- Choose silicone insulators;
- Enable, with regard to the maximum values of the discharge currents and the voltage application times, an operating margin taking into account the insulators behavior over the entire range of the operating insulators voltages;
- Increase immunity against electric discharge while designing and maintaining electrical insulators in good surface condition;
- Reduce the diameter of the HV electrode.

REFERENCES

[1] S. S. Kulkarni, P. C. Tapre, **"Analysis of electric field stresses on spacers in GIS for different ratings"**, *in 2017 International Conference on Intelligent Computing and Control Systems (ICICCS)*, Madurai, India, pp. 295-300, 2017.

[2] T. S. Sudarshan and R. A. Dougal, "**Mechanisms of surface flashover along solid dielectrics in compressed gases: A review"**, *IEEE Transactions on Electrical Insulation*, Vol. EI-21, No. 5, 1986, pp. 727 – 46.

[3] A. H. Cookson, **"Gas-Insulated Cables"**, *IEEE Transactions on Electrical Insulation*, Pittsburgh, Vol. 20, No. 5, pp. 859 – 890, 1985.

[4] W. Pengfei, D. Quanlin, W. Guozeng, L. Junbiao, L. Wenping, **"Practical design of triple junction for a 90 kV electron gun"**, IEEE Transactions on Dielectrics and Electrical Insulation, Vol. 26 , No. 4, pp. 1043 – 1047, 2019.

[5] R. Kyosu, Y. Yamano, N. Asari, T. Shioiri, K. Matsuo, **"Vacuum Surface Flashover Characteristics of the Alumina Insulator with Different Metallized Edge Conditions"**, *in 2018 28th International Symposium on Discharges and Electrical Insulation in Vacuum (ISDEIV)*, Greifswald, Germany, pp. 159-162, 2018.

[6] J. H. Song, J. Y. Kim, B. Y. Seok, Y. C. Choi, **"Evaluation of discharge characteristics on the triple junction for development of the Gas-Insulated Switchgear"**, *in 2012 15th International Conference on Electrical Machines and Systems (ICEMS)*, Sapporo, Japon, 2012.

[7] A, Goldman, M. Goldman, E. Odic and Ph. Dessante,

"Partial discharges inception and ageing effects in a gas insulated HV equipment", *in 2008 17th International Conference on Gas Discharges and Their Applications*, Cardiff, UK, 2008.

[8] M. Toepler, **"T~ber die physikalischen Grundgesetze der in der Isolatorentechnik auftretenden elektrischen Gleiterscheinungen"**, *Arch. Elektrotech*, Vol. 157, No. 10, 1921.

[9] K. R. Venna, H. H. Schramm, **"Simulation Analysis on Reducing the Electric Field Stress at the Triple Junctions & on the Insulator Surface of the High Voltage Vacuum Interrupters"**, *in XXVI International Symposium On Discharges and Electrical Insulation in Vacuum (ISDEIV)*, Mumbai, India, pp. 53-56. 2014.

[10] A. Sobota, A. Lebouvier, N. J. Kramer, E. M. Veldhuizen, W. W. Stoffels, F. Manders and M. Haverlag, **"Speed of streamers in argon over a flat surface of a dielectric"**, *Journal of Physics D: Applied Physics*, Vol. 42, 2009.

[11] J. E. Lauer, C. J. Lauer, **"Electron avalanche on a dielectric-vacuum interface"**, *IEEE Transactions on Dielectrics and Electrical Insulation*, Vol. 24, No. 2, pp. 1295 - 1299, 2017.

[12] W. Pengfei, D. Quanlin, W. Guozeng, L. Junbiao, L. Wenping, **"Practical design of triple junction for a 90 kV electron gun"**, *IEEE Transactions on Dielectrics and Electrical Insulation*, Vol. 26, No. 4 , pp. 1043 – 1047, 2019.

[13] L. Zeghichi, L. Mokhnache, M. Djebabra, **"The Monte Carlo Method for the Study of an Electrical Discharge"**, *in 2013 IEEE International Conference on Solid Dielectrics*, Bologna, Italy, pp. 636 – 639, 2013.

[14] Li. Junhao, Si. Wenrong, Y. Xiu, L. Yanming, **"Partial discharge characteristics over differently aged oil/pressboard interfaces"**, *IEEE Transactions on Dielectrics and Electrical Insulation*, Vol. 16, No. 6 , pp. 1640 – 1647, 2009.

[15] T. S. Sudarshan and R. A. Dougal, **"Mechanisms of Surface Flashover Along Solid Dielectrics in Compressed Gases: a Review"**, *IEEE Transactions on Electrical Insulation*, Vol. EI-21, No. 5, pp. 727 – 746, 1986.

[16] A, Zeeshan , R. C. Mojtaba, Y. Kamran, K. Joni, **"Multivariate Time Series Modeling for Long Term Partial Discharge Measurements in Medium Voltage XLPE Cables"**, *in 2019 Electrical Insulation Conference (EIC)*, Calgary, Alberta, Canada, pp. 344 – 347, 2019.

[17] D. E. Bruno, E. Barca, R. M. Goncalves, H. A. de A. Queiroz, L. Berardi, G. Passarella, **"Linear and evolutionary polynomial regression models to forecast coastal dynamics"**, *Comparison and reliability assessment*, Geomorphology, Vol. 300, pp. 128–140, 2018.

[18] D. J. Olive, **"Multiple linear regression"**, *Linear Regression*, Springer, Cham, pp. 17-83, 2017.

[19] E. A. Khailenko, E. P. Arhipenko, **"Development of Robust Methods for Estimating Parameters of Polynomial Structural Dependencies"**, *in 2018 XIV International Scientific-Technical Conference on Actual Problems of Electronics Instrument Engineering (APEIE)*, Novosibirsk, Russia, pp. 115-117, 2018.

[20] A. F. L. Lopera, F. Bachoc, N. Durrande, J. Rohmer, D. Idier, O. Roustant, "**Approximating Gaussian Process Emulators with Linear Inequality Constraints and Noisy Observations via MC and MCMC",** in book: *Monte Carlo and Quasi-Monte Carlo Methods*, Rennes, France, pp. 363-381, 2020.

[21] S. Da. Veiga, A. Marrel, **"Gaussian process regression with linear inequality constraints"**, *Reliability Engineering and System Safety*, Vol. 195, pp. 1 -13, 2020.

[22] D. W. Marquardt, **"An algorithm for least-squares estimation of nonlinear parameters"**, *Journal of the Society for Industrial and Applied Mathematics*, Vol. 11, No. 2, pp. 431 – 441, 1963.

[23] M. A. HANDALA and O. LAMROUS, **"Surface degradation of styrene acrylonitrile exposed to corona discharge"**, *EUROPEAN TRANSACTIONS ON ELECTRICAL POWER*, Vol. 18, pp. 494 – 505, 2008.

[24] J. Martinez-Vega, **"Dielectric materials for electrical engineering 1: properties, aging and modeling"**, *Hermes Science*/Lavoisier, Paris, France, 2007. (In French)

[25] J. P. Habas, J. M. Arrouy, F. Perrot, **"Effects of electric partial discharges on the rheological and chemical properties of polymers used in HV composite insulators after railway service"**, *IEEE Transactions on Dielectrics and Electrical Insulation*, Vol. 16, No. 5, pp. 1444 – 1454, 2009.

[26] P. Robert, **"Electrotechnical materials"**, *Collection: electricity treaty*, 1999.

[27] M. Lévesque, É. David, C. Hudon and M. Bélec, **"Effect of surface degradation on slot partial discharge activity"**, *IEEE Transactions on Dielectrics and Electrical Insulation*, Vol. 17, No. 5, pp. 1428 – 1440, October 2010.

[28] J. Lewis, T. S. Sudarshan, J. E. Tompson, D. Lee, R. A. Dougal, **"Pre-breakdown and breakdown phenomena of electric surface in vacuum and nitrogen gaz stressed by 60 Hz voltage"**, *in IEEE Conference Record-International Phenomena in Practical Systems*, Gaithsburg, MD, USA, pp. 19-20, 1988.

[29] M. U. Siddiqui, N. Hershkowitz, R. Bonazza, **"An investigation of micron diameter exposed-electrode single barrier dielectric barrier discharges"**, *in Abstracts IEEE International Conference On Plasma Science 2011*, Chicago, IL, USA, pp. 1-1, Jun. 2011.

[30] G. D'Urso and C. Ravasio, **"The effects of electrode size and discharged power on micro-electro-discharge machining drilling of stainless steel"**, *Advances in Mechanical Engineering*, Vol. 8, No. 5, pp. 1-12, 2016.

[31] M. N. Lyulyukin, A. S. Besov, A.V. Vorontsov, **"The Influence of corona Electrodes Thickness on the Efficiency of Plasma chemical Oxidation of Acetone"**, *Plasma Chem Plasma Process*, Vol. 31,

pp. 23-39, 2011.

[32] A. Capozzoli, D. Grassi, F. Causone, **"Estimation models of heating energy consumption in schools for local authorities planning"**, *Energy Build*, Vol. 105, No. 15, pp. 302-313, 2015.

[33] Jagannath, T. Tsuchido, **"Validation of a polynomial regression model: the thermal inactivation of Bacillus subtilis spores in Milk"**, *Letters in Applied Microbiology*, Vol. 37, pp. 399 –404, 2003.

[34] L. Martino, V. Laparra, G. Camps-Valls, **"Probabilistic Cross-Validation Estimators for Gaussian Process Regression"**, *in 2017 25th European Signal Processing Conference (EUSIPCO)*, Kos, Grèce, pp. 823-827.8, 28 août-2 septembre 2017.